
Concise Reasoning via Reinforcement Learning

Mehdi Fatemi*, Banafsheh Rafiee*, Mingjie (Mike) Tang, and Kartik Talamadupula

Wand AI

Abstract

Despite significant advancements in large language models (LLMs), a major drawback of reasoning models is their enormous token usage, which increases computational cost, resource requirements, and response time. In this work, we revisit the core principles of reinforcement learning (RL) and, through mathematical analysis, demonstrate that the tendency to generate lengthy responses arises inherently from RL-based optimization during training. This finding questions the prevailing assumption that longer responses inherently improve reasoning accuracy. Instead, we uncover a natural correlation between conciseness and accuracy that has been largely overlooked. We show that introducing a secondary phase of RL training, using a very small set of problems, can significantly reduce chains of thought while maintaining or even enhancing accuracy. Additionally, we demonstrate that, while GRPO shares some interesting properties of PPO, it suffers from collapse modes, which limit its reliability for concise reasoning. Finally, we validate our conclusions through extensive experimental results.

1 Introduction

Reasoning models have gained significant importance in both research and products, demonstrating remarkable performance in various domains. This success is largely attributed to extensive reinforcement learning (RL) [1] post-training applied to a base model, which is initially trained through supervised learning for token completion. During RL training, the model is exposed to a diverse set of reasoning-related problems, along with their corresponding final answers. Notably, using a complete solution as the training target is not required in RL; instead, the model explores the response space, similar to how an RL agent learns to play a video game. This process fundamentally differs from the (supervised) training phase designed for human alignment, commonly referred to as reinforcement learning from human feedback (RLHF), where the objective is to select responses that align with human preferences among multiple model-generated alternatives.

A key phenomenon observed during RL post-training is the emergence of an “aha moment” [2]. This refers to an inflection point where the model begins exhibiting self-correction behaviors, as seen in responses like “*We must have made a mistake, let’s try again.*” Crucially, this behavior is not explicitly programmed but emerges naturally as the model explores the response space. Prior research has found a distinct pattern following this moment: response lengths tend to increase significantly, accompanied by improvements in overall accuracy [2–4]. Even with a lack of clear understanding of why this happens, this phenomenon has led many to push for longer responses, leveraging additional training and computational resources in the hope of further enhancing accuracy.

We argue that the observed gains in accuracy are distinct from the tendency to generate longer responses. The latter stems primarily from RL’s loss optimization, not from an inherent requirement for extended responses. This view also resolves the apparent paradox that, in both reasoning and non-reasoning models, correct responses to reasoning-intensive tasks are often shorter than incorrect

*Equal contribution. Correspondence to: mehdi@wand.ai and banafsheh.rafiee@wand.ai

ones. The model’s inclination toward lengthier outputs is not a deliberate reasoning strategy but a side effect of minimizing loss.

Moreover, a critical but often overlooked observation is that RL post-training on moderate-size datasets from domains like mathematics often leads to an initial decrease in response length with no negative impact on the accuracy [5, 6]. This suggests that many tokens in the produced chain of thought may not be needed. Additionally, examining the chain of thought in reasoning models, such as DeepSeek’s R1 [2], reveals a significant degree of redundancy, repetition, and irrelevant artifacts, including unnecessary code generation and even multilingual output.

This observation raises a fundamental question: Can reasoning models be further optimized through RL training to produce systematically more concise chains of thought without sacrificing accuracy? To this end, and in light of our theoretical analysis, we propose a *two-phase RL training* paradigm designed to first enhance the reasoning capabilities of the base model and then enforce conciseness.

- Phase 1: Initial training on challenging problems to improve the model’s reasoning capacity;
- Phase 2: Targeted training on problems that are at least occasionally solvable to enforce conciseness while preserving or enhancing accuracy.

Both phases can be trained on a small problem set, but the second is key to producing concise responses. Our approach offers a direct alternative to models such as DeepSeek’s R1, yielding significantly shorter responses while maintaining accuracy and in some cases even improving it. It is cost-effective, requires minimal training, and improves computational efficiency, resource use, and response time. Additionally, we present the following key findings.

1. **Correlation of Conciseness and Accuracy:** We show that, during inference of both reasoning and non-reasoning models, *concise reasoning* tends to strongly correlate with higher accuracy.
2. **Analysis of PPO Loss Function Dynamics:** We present a mathematical analysis establishing the link between response correctness and PPO’s loss function. Specifically, we show that incorrect answers tend to drive longer responses, while correct ones encourage brevity.
3. **Analysis of GRPO Loss Function Dynamics:** We show that while GRPO encourages longer responses when facing negative advantage and halts growth and promotes conciseness when facing positive advantage, it suffers from collapse modes, making it ineffective in enforcing conciseness.
4. **Limited Data:** We show that RL post-training phases are effective even with remarkably small datasets, a result that defies current trends in the literature and proves viable for resource-constrained scenarios, as confirmed by our experiments.

2 Response Length vs. Accuracy

A crucial yet often overlooked phenomenon is that in both reasoning and non-reasoning models, with or without RL training, brevity and accuracy are strongly correlated (see Table 1). Moreover, as reported in previous works [5, 6], RL post-training often produces significantly shorter responses, even without explicit penalties for length, while still preserving or improving correctness. This effect is particularly evident in the early stages of training.

Model	MATH500		AIME’24		MMLU-STEM	
	Correct	Incorrect	Correct	Incorrect	Correct	Incorrect
R1-Distill-Qwen-1.5B	3518 ₃₃₁₄	11519 ₆₈₆	7462 ₇₂	14269 ₁₆₈	1577 ₉₇₅₆	3431 ₁₄₃₈₈
R1-Distill-Qwen-7B	3204 ₁₈₅₈	10436 ₁₄₂	6953 ₆₄	14576 ₅₆	818 ₆₁₂₁	1377 ₅₉₅₁
Qwen2.5-Math-1.5B-Inst	477 ₅₉₄₆	815 ₂₀₅₄	779 ₅₁	989 ₄₂₉	382 ₂₇₂₇₉	460 ₂₁₀₀₉
Phi-4	529 ₆₃₉₇	1107 ₁₆₀₃	932 ₈₀	1333 ₄₀₀	383 ₁₁₄₁₇	406 ₃₆₈₇₁

Table 1: Average response length for correct and incorrect answers across different models and benchmarks. The blue subscripts indicate the number of samples used to compute the averages.

These observations are in sharp contrast with the widespread belief that very long chains of thought are inherently necessary to achieve higher accuracy [2–4]. A related explanation for why long

responses may reduce accuracy is the notion of deadends—states where reaching the correct answer becomes unlikely [7–9]. When the risk of a deadend is low, generating more text can help find a solution. However, when the risk is higher, longer responses increase the likelihood of failure, potentially outweighing any benefit. In practice, deadends still occur in LLMs despite strong sampling techniques, often appearing as endless repetition or a complete detour from the intended reasoning.

Observing that long responses are not necessarily correlated with accuracy, a key question remains: When and why do LLMs, trained with RL, tend to increase response length? To answer this question, we return to RL fundamentals, formalizing each reasoning problem as an MDP in the next section.

3 Each Reasoning Problem is an MDP

Each reasoning problem (e.g., a math problem) fundamentally constitutes a Markov Decision Process (MDP) [10] rather than a mere static sample. An MDP consists of a state space \mathcal{S} , an action space \mathcal{A} , a transition function T , a reward function R , an initial state distribution \mathcal{P}_0 , and a discount factor γ . In language modeling, the state at each token position k consists of all tokens (or their embeddings) up to and including k , as well as any contextual information such as the problem statement. The action space corresponds to the vocabulary of possible tokens. The transition function deterministically appends new tokens to the sequence. The reward function is zero for all steps except the final one, where correctness is evaluated based on final answer and formatting. The initial state depends on the prompt, which may include problem statements and directives (e.g., "Solve step by step and enclose the final answer in a box."). The RL objective is to maximize the expected return, referred to as the value function and denoted by $V(s)$, where return is defined as the sum of future rewards discounted by γ . It is common practice in LLM post-training to set γ to 1.

Solving a problem when only the final answer is given requires a base model capable of occasional correct solutions, akin to an agent playing an interactive game. When training on multiple problems, the overall MDP consists of multiple initial states with an updated reward function. Adding more problems modifies P_0 and R but retains the fundamental MDP structure. This introduces two considerations: (1) A larger set of problems increases the MDP complexity, which may lead to greater generalization of the learned skills. (2) In principle, a small set of problems (even a single one) should be sufficient for RL training to take effect, though this may raise concerns about overfitting.

Overfitting is a concern in supervised learning, where models memorize specific examples rather than generalizing. In contrast, online RL does not suffer from this issue. Unlike supervised learning, which relies on static training data, online RL continually generates new response trajectories, enabling the model to refine its reasoning dynamically. Moreover, online RL does not merely imitate predefined solutions; it actively explores diverse reasoning strategies and reinforces those that lead to correct answers. Two key mechanisms contribute to this robustness: (1) sampling techniques, such as non-zero temperature, ensure variation in generated responses, and (2) continual model updates during training introduce new response distributions over time, preventing stagnation and overfitting. This explains why RL training on a small set of problems is expected to remain effective. To the best of our knowledge, applying RL training to extremely small datasets has not been explored in the literature, making it a novel contribution of this work.

Beyond data size, we emphasize that *the sole objective* of RL is to minimize loss, which corresponds to maximizing expected return. From this perspective, any noticeable change in response length during RL training must be driven by loss minimization rather than the model’s inherent inclination toward more extensive reasoning. This phenomenon is fundamentally different from reward hacking, where an agent exploits unintended shortcuts to maximize return without genuinely solving the task. In contrast, what we described above doesn’t stem from manipulating poorly designed or hidden rewards; it emerges directly from how the loss is computed from the reward.

4 PPO Impact on Response Length

To study the relation between response length and RL loss, we trained DeepSeek-R1-Distill-Qwen-1.5B using Proximal Policy Optimization (PPO) [11]. Training was performed on only 4 problems from the OlympiadBench dataset [12] (see Appendix A.3). These problems were specifically chosen because the base model consistently failed to solve them even with extensive sampling, leading to a *constant terminal reward* of -0.5 .

The context size was limited to 20K tokens, and we plot policy loss against response length in Figure 1. The plot clearly shows a strong correlation: as response length increased, loss consistently decreased. This provides direct evidence that loss minimization, rather than any intrinsic tendency of the model to produce longer responses, is the primary force driving response length growth. Next, we present a mathematical analysis explaining why this occurs.

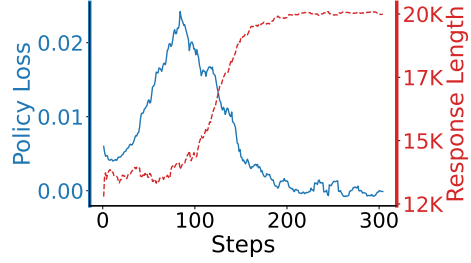


Figure 1: **Effect of loss on response length.** The curves are smoothed using a 10-step moving average.

Using generalized advantage estimation (GAE) [13], the advantage function is estimated as a λ -weighted sum of step-wise TD-errors, similar to eligibility traces in value estimation [1, 14]. PPO then uses GAE to estimate the loss for policy training. In practice, PPO is often used with $\gamma = 1$ and $\lambda = 0.95$.

Consider a response of length T (with token indices from 0 to $T - 1$), where a terminal reward $r \neq 0$ is applied only at the final step, $T - 1$. Let $\gamma = 1$. In PPO, per-token loss is averaged over the full response length T . We assume $|V(s_{t+1}) - V(s_t)| \leq \epsilon \quad \forall t$. This is expected since the value network’s output spaces is by design bounded and Lipschitz continuous. We show that when $\lambda < 1$, PPO favors shorter responses if $r > 0$ and longer responses if $r < 0$. Importantly, we demonstrate that setting $\lambda = 1$ may introduce an undesirable bias toward shorter responses regardless of their correctness and significantly amplifies noise, with noise scaling linearly in response length.

By design, $r_t = 0$ for $t < T - 1$, and $r_t = r$ for $t = T - 1$. With the temporal-difference error $\delta_t = r_t + V(s_{t+1}) - V(s_t)$, and $\gamma = 1$, the GAE advantage for token t is $\hat{A}_t = \sum_{l=0}^{T-t-1} \lambda^l \delta_{t+l}$. The PPO loss is proportional to the negative average of \hat{A}_t ’s, weighted by a positive coefficient derived from the clipped importance sampling ratio and additional positive regularization terms. Thus, the per-token loss satisfies $L_t \propto -\hat{A}_t$, and the overall loss minimized by the optimizer is:

$$L_{\text{avg}} = \frac{1}{T} \sum_{t=0}^{T-1} L_t \propto -\frac{1}{T} \sum_{t=0}^{T-1} \hat{A}_t$$

We state the following result characterizing the asymptotic behavior of the average PPO loss under GAE:

Theorem 1 [PPO Loss under GAE]: Let \hat{A}_t denote the GAE with parameter $\lambda \in [0, 1]$, and $r_t = 0$ for $t < T - 1$, and $r_{T-1} = r$, and assume the value function satisfies $V(s_T) = 0$. Let the TD errors be $\delta_t = r_t + V(s_{t+1}) - V(s_t)$, and define $R := r - V(s_{T-1})$, where $\text{sign}(R) = \text{sign}(r)$. Let the TD error satisfy $|\delta_k| \leq \epsilon$ for $k < T - 1$. Then, the average PPO loss satisfies:

$$L_{\text{avg}} \propto \begin{cases} -\frac{R}{T(1-\lambda)} + O\left(\frac{\epsilon}{1-\lambda}\right) & \text{if } \lambda < 1 \\ -R + O\left(\frac{\epsilon \cdot T}{2}\right) & \text{if } \lambda = 1 \end{cases}$$

Interpretations. Our results lead to the following key points:

- **For $\lambda < 1$**
 - The average error term remains bounded by a constant as $O(\epsilon/(1-\lambda))$.
 - If $R < 0$: with high probability $L_{\text{avg}} > 0$, and its magnitude decreases as T increases. That is, longer responses receive smaller loss, so PPO favors them more.
 - If $R > 0$: with high probability $L_{\text{avg}} < 0$, and its magnitude increases as T decreases. That is, shorter responses receive smaller (more negative) loss, so PPO favors them more.
 - Our numerous experiments confirm that consistently negative rewards yield positive loss (e.g., Figure 1), while predominantly positive rewards yield negative loss.
- **For $\lambda = 1$**
 - The average error scales linearly with T , making PPO highly sensitive to value estimation errors, leading to significantly slower, inefficient, or unstable training (see Appendix Fig. 7).
 - It could be difficult to enforce long responses even when the answer is consistently incorrect.

- The **return** is computed as $\hat{A}_t + V_t = r - V_{T-1} + V_t + \sum_{l=1}^{T-t-2} \delta_{t+l}$ and used as the target for V_t in the next iteration. When $r < 0$, the positive $V_t - V_{T-1}$ pushes the target upward, causing overflow, especially for early tokens. When $r > 0$, it can pull the target downward, leading to underflow (see Appendix Figs. 6 and 7). Note that when $\lambda < 1$, V_t is heavily discounted.

Remark. For $\gamma < 1$, including γ in the analysis has two effects: (1) similar to λ , it directly affects the loss, and (2) it modifies the TD errors, introducing a lower bound on ϵ that may degrade training performance. Thus, we recommend using λ instead (see Appendix A.1 for more details).

5 GRPO Impact on Response Length

In the case of GRPO [15], loss is calculated from the following formula (note the negative sign):

$$L_{\text{GRPO}}(\pi_\theta) = -\mathbb{E}_{q \sim p_Q, \{o^{(i)}\}_{i=1}^G \sim \pi_{\theta_{\text{old}}}(\cdot|q)} \frac{1}{G} \sum_{i=0}^{G-1} \frac{1}{|o^{(i)}|} \sum_{t=0}^{|o^{(i)}|-1} \left(\min \left[\frac{\pi_\theta(o_t^{(i)}|q, o_{<t}^{(i)})}{\pi_{\theta_{\text{old}}}(o_t^{(i)}|q, o_{<t}^{(i)})} \hat{A}_t^{(i)}, \text{clip} \left(\frac{\pi_\theta(o_t^{(i)}|q, o_{<t}^{(i)})}{\pi_{\theta_{\text{old}}}(o_t^{(i)}|q, o_{<t}^{(i)})}, 1 - \epsilon, 1 + \epsilon \right) \hat{A}_t^{(i)} \right] \right) \quad (1)$$

where π_θ and π_{old} are the main policy and the one before the update, and advantage is given by

$$\hat{A}_t^{(i)} = \frac{r(q, o^{(i)}) - \text{mean}(\{r(q, o^{(1)}), \dots, r(q, o^{(G)})\})}{\text{std}(\{r(q, o^{(1)}), \dots, r(q, o^{(G)})\})} \quad (2)$$

where $o^{(i)}$ and $o_t^{(i)}$ denote the i -th response and the t -th token in the i -th response, respectively. Liu et al. [16] argued that the presence of $|o^{(i)}|$ in the denominator biases the model by encouraging longer responses when the advantage is negative and vice versa. To address this perceived issue, they proposed removing $|o^{(i)}|$ from the denominator. Unfortunately, this interpretation misses important details. As response length increases, both the numerator and the denominator grow, not just the denominator. Thus, the relationship between response length and loss is more nuanced than they imply. We present an alternative argument showing that the GRPO loss encourages longer responses for negative advantages and shorter responses for positive ones. However, we also show that GRPO has notable shortcomings, casting doubt on its effectiveness, particularly for improving conciseness.

Two key observations: (1) by definition, advantage is independent of token position t , so the subscript is redundant and can be moved outside the inner sum; (2) although GRPO typically uses non-negative rewards, \hat{A} reverses their effect. With some responses labeled positive and others zero, the mean in Equation (2) lies between 0 and 1, yielding $\hat{A} > 0$ for correct responses and $\hat{A} < 0$ for incorrect ones. This also highlights another similarity between GRPO and PPO’s common practice, where incorrect responses incur negative rewards. The following theorem summarizes GRPO’s core behaviour.

Theorem 2 [GRPO Prolivity]: Let π_θ and $\pi_{\theta_{\text{old}}}$ be the current and old policies in GRPO training. Consider a sampled response ending in a terminal token τ , with advantage \hat{A} . Then, (1) if $\hat{A} < 0$, decreasing $\pi_\theta(\tau)$ reduces the loss; and (2) if $\hat{A} > 0$, increasing $\pi_\theta(\tau)$ reduces the loss.

This result shows that $\hat{A} < 0$ is a sufficient condition for encouraging longer responses, a phenomenon widely observed by practitioners. When $\hat{A} > 0$, it implies a higher chance of termination at the current position once updated, but it does not favor shorter responses among multiple correct completions. To address this, we present a general result, mainly relevant to GRPO, focusing on what happens when *two correct responses differ in length*. Without loss of generality, we assume the first token of each response acts as the trigger guiding the model toward that sequence. To simplify notations, we remove conditioning from policies. From (1), for any *correct* response i , we have

$$L^{(i)} = -\hat{A}^{(i)} \cdot \frac{1}{|o^{(i)}|} \sum_{t=0}^{|o^{(i)}|-1} \min(\rho_t^{(i)}, 1 + \epsilon), \quad \rho_t^{(i)} = \frac{\pi_\theta(o_t^{(i)})}{\pi_{\theta_{\text{old}}}(o_t^{(i)})}$$

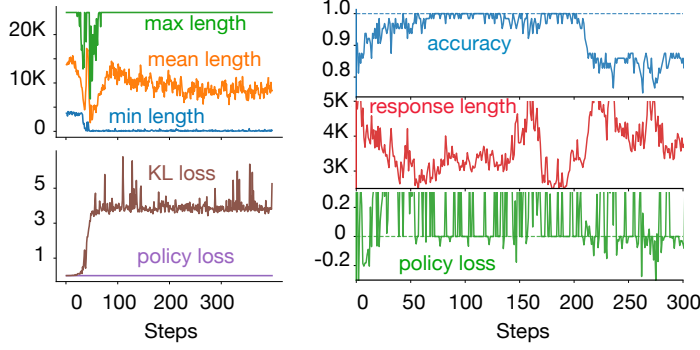


Figure 2: **GRPO on unsolvable and easy problems.** **Left:** On unsolvable problems, both policy loss and reward remained zero and the KL resulted in the collapse of **min** response length. **Right:** On easy problems, the policy loss dropped to zero when accuracy hit one, disrupting the learning process.

Theorem 3 [General Conciseness]: Let π_θ be a “softmax” policy over a vocabulary of size K . Let $o_0^{(S)}$ and $o_0^{(L)}$ denote the first tokens of two responses generated by $\pi_{\theta_{\text{old}}}$ leading to sequence lengths T_S and $T_L > T_S$, respectively. Assume: (1) both responses share the same positive advantage $\hat{A} > 0$; and (2) the importance sampling ratios satisfy $\rho_0^{(S)}, \rho_0^{(L)} < 1 + \epsilon$. Then,

1. For token k in vocabulary, the gradient norm induced by the softmax layer w.r.t. the logits z is

$$f(o_t^{(i)} = k) := \left\| \nabla_z \log \pi_\theta(o_t^{(i)} = k) \right\| = \left[(1 - \pi_\theta(o_t^{(i)} = k))^2 + \sum_{j \neq k} \pi_\theta(o_t^{(i)} = j)^2 \right]^{\frac{1}{2}}$$

2. $\left\| \nabla_\theta L^{(S)}(o_0^{(S)}) \right\| > \left\| \nabla_\theta L^{(L)}(o_0^{(L)}) \right\|$ iff $\rho_0^{(S)} f(o_0^{(S)}) > \frac{T_S}{T_L} \tilde{\kappa} \rho_0^{(L)} f(o_0^{(L)})$, with $\tilde{\kappa} > 0$.
3. This result is invariant under softmax temperature rescaling.

Interpretations.

- Under similar conditions (i.e., when $\pi_\theta(o_0^{(S)}) = \pi_\theta(o_0^{(L)})$ and $\rho_0^{(S)} = \rho_0^{(L)}$), the inequality generally holds because $T_S/T_L < 1$; hence, the shorter response receives stronger reinforcement (note that $L < 0$ for both responses since $\hat{A} > 0$).
- The update almost surely favors shorter responses when $T_L \gg T_S$, or $\rho_0^{(S)} f(o_0^{(S)}) \gg \rho_0^{(L)} f(o_0^{(L)})$.
- If either $\rho_0^{(S)}$ or $\rho_0^{(L)}$ hits $1 + \epsilon$, the gradient is clipped to zero, preventing further preference.
- The possible range for $\tilde{\kappa}$ depends on the Jacobian’s singular values, but experimental results indicate that $\tilde{\kappa}$ has a minor effect on the inequality, as conciseness still occurs under GRPO.

The Collapse of GRPO

In Appendix A.4, we show that the advantage function in GRPO admits the following closed form:

$$\hat{A} = \frac{r - \mu}{\sigma} = \begin{cases} \sqrt{(N - k)/k}, & \text{if } r = 1 \\ -\sqrt{k/(N - k)}, & \text{if } r = 0 \end{cases} \quad (3)$$

where k denotes the number of correct responses within a group of size N . Notably, \hat{A} is invariant under reward scaling. Expression (3) induces $\hat{A} = 0$ whenever the group is entirely correct or entirely incorrect. This structural property has critical implications for the learning dynamics of GRPO.

First, unsolvable problems: When problems are unsolvable, GRPO behaves differently from PPO. Since $\hat{A} = 0$, Theorem 2 does not apply and the loss is dominated by the KL term, which discourages deviation from the base model. To explore this further, we trained GRPO on four OlympiadBench problems using DeepSeek-R1-Distill-Qwen-1.5B (Figure 2, left). Surprisingly, the model quickly converged to extremely short outputs (fewer than 80 tokens), likely because shorter responses incur lower KL penalties than longer ones.

Second, fully solvable problems: A similar failure mode arises when problems are consistently solvable. As accuracy hits 1, the estimated advantage \hat{A} converges to zero, causing the policy loss

to vanish. In this regime, the KL divergence term once again dominates the loss. We observed this effect by training GRPO on eight problems from the MATH dataset (Figure 2, right). Once the model consistently solved all examples, progress stalled. In large datasets, this issue is often masked, as training batches are likely to include at least some partially solved or unsolved examples with non-zero advantage. However, in smaller or skewed datasets dominated by fully solvable problems, the advantage collapses across the board, reactivating the KL penalty as the primary learning signal. As a result, Theorem 3 becomes inapplicable, and GRPO loses its conciseness-inducing effect. While GRPO typically outperforms PPO in early training, this advantage can erode over time unless the KL term is carefully managed or adaptively reweighted.

Crucially, PPO does not suffer from these issues. In PPO, response length directly affects the advantage, whereas in GRPO, the advantage is fixed. This difference alone makes PPO more effective at promoting conciseness. Combined with the limitations noted above, these factors support using PPO over GRPO as a more robust method, especially when conciseness is a key objective.

6 A Two-Phase Reinforcement Learning Strategy

Our analysis highlights key dynamics in response length during RL training. When models are trained on exceptionally difficult problems, response length tends to increase, as longer outputs are more likely to reduce the loss amid predominantly negative rewards. Conversely, for occasionally solvable problems, response length typically decreases. In large-scale settings, this behavior becomes complex and closely tied to problem difficulty. As more problems become at least occasionally solvable, we expect average response length to eventually decrease.

In practice, RL training data often contains difficult problems. As long as some problems consistently yield negative rewards, the tendency toward longer responses can persist, especially early in training or once easier problems are mastered. This push towards verbosity, combined with LLMs’ strength in producing coherent text, may contribute to the “aha moment,” producing elaborate but not necessarily more accurate answers. It is also important to note that longer responses do not imply persistent failure. The model may reach correct answers simply by continuing its chain of thought. When this happens, RL reinforces success regardless of token count, which explains why accuracy can improve even amid growing verbosity. The key point is that verbosity is a consequence of RL minimizing its loss in the face of negative rewards, and it is this verbosity that may occasionally lead to improved accuracy, which then would be reinforced, not the other way around.

If the dataset contains an excessive number of unsolvable problems, the transition from promoting longer responses to encouraging conciseness can be significantly delayed and costly. To overcome this, we propose a novel approach: enforcing conciseness through a subsequent phase of RL training with a dataset of occasionally solvable problems. This structure introduces a two-phase RL training:

1. In the first phase, the model is trained on challenging problems. This phase aims to enhance the model’s problem-solving capacity, with an expected increase in response length as PPO/GRPO mostly encounters wrong answers, driving the model toward longer responses. Notably, this first phase can also be seen as the RL training of off-the-shelf reasoning models.
2. In the second phase, training continues on problems with non-zero p_a (occasionally solvable). This phase enforces conciseness while preserving or even enhancing accuracy. Notably, as we will see, it also substantially improves the model’s robustness to lowering the temperature, ensuring remarkable performance even with limited sampling.

A critical insight from the MDP perspective is that effective RL training can be achieved even with a small problem set, though at the cost of possibly reduced generalization. In particular, in the second phase of training, where the model has already developed generalization capabilities, PPO can be applied to a minimal dataset consisting of only a few problems.

7 Experimental Results

In our experiments, we broadly show that our two-phase reinforcement learning strategy leads to significant improvements across various models. We begin by examining the impact of problem difficulty level (p_a) and demonstrate how RL can influence response length depending on the

solvability of training problems. Next, we demonstrate that a second phase of training on R1 models, using only eight problems, achieves significantly more concise reasoning across various benchmarks, while preserving (even improving) accuracy. Additionally, this second phase of RL post-training substantially enhances model robustness under reduced sampling intensity. Finally, revisiting the first phase, we establish that *non-reasoning models* can be vastly improved through minimal-scale RL training. These results highlight the broad applicability and efficiency of our approach.

We used DeepSeek-R1 models distilled on Qwen models as our base and applied RL post-training to the 1.5B and 7B variants. During each training cycle, the model generated eight independent responses per training example, which were scored based on their format and the correctness of the final answer. For PPO, we used the following reward scheme: +1 if the final answer was correct and enclosed in a box; -0.5 if the answer was boxed but incorrect; and -1 if no boxed answer was provided. For GRPO, we used a simpler reward scheme: +1 for a correct and boxed final answer, and 0 otherwise. (See Appendix A.6 for more information about the experimental setup.)

7.1 Impact of Problem Difficulty on Accuracy-Length Correlation

In this section, we present experimental results supporting our claim that RL training on occasionally solvable problems leads to shorter response lengths. This reduction correlates with problem difficulty and an increased probability of arriving at a correct answer (p_a), which in turn promotes more concise responses. We considered 3 sets of training examples, each containing 4 problems from the AIME’24 dataset. To estimate problem difficulty, we evaluated the base model using 64 samples per problem and temperature 0.6. The average p_a for the three sets, from easiest to hardest, was 0.375, 0.25, and 0.16, respectively. Figure 3 shows the accuracy and response length over training steps for both cases of PPO and GRPO. Across all problem sets and algorithms, improvements in accuracy coincided with reductions in response length, indicating that as the model became more accurate, its responses became shorter.

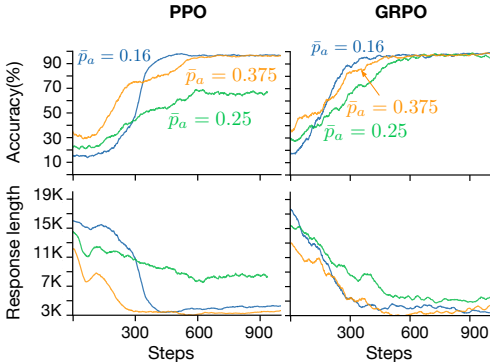


Figure 3: **Impact of difficulty levels.** Curves are smoothed with a 50-step moving average. Accuracy improvements consistently aligned with shorter response lengths across all problem sets and training algorithms.

7.2 Decrease in Response Length

In this section, we demonstrate the effect of RL post-training using eight training examples from the training subset of MATH dataset [17] on reducing response length. We report PPO results, as GRPO performs unreliably on easy problems due to the collapse discussed in Section 5. (See Appendix A.10 for GRPO results). Although training was conducted exclusively on examples from the MATH dataset, we evaluated the models on AIME 2024 and AMC 2023 as well. For evaluation, we generated four samples per query using a temperature of 0.6 and top-p of 0.95.

Figure 4 (left) illustrates the accuracy and response length of the post-trained models over training steps, evaluated on *test* datasets of AIME 2024, AMC 2023, and MATH-500. Our results show that the response length decreased significantly, while accuracy remained stable across benchmarks and model sizes. To investigate whether reducing response length through RL post-training generalizes to other domains, we evaluated the 1.5B and 7B models trained on the eight training examples from the training subset of MATH dataset using the MMLU benchmark. The MMLU benchmark includes multiple-choice questions across 57 diverse subjects. For this evaluation, we specifically used MMLU-STEM, which focuses on science and engineering subjects such as physics, biology, electrical engineering, and computer science. This subset contains 3018 distinct problems. The results are illustrated in Figure 4 (right). As with the math domains, PPO post-training led to shorter response lengths on MMLU. Surprisingly, even with training on just eight examples, RL post-training also resulted in an accuracy improvement.

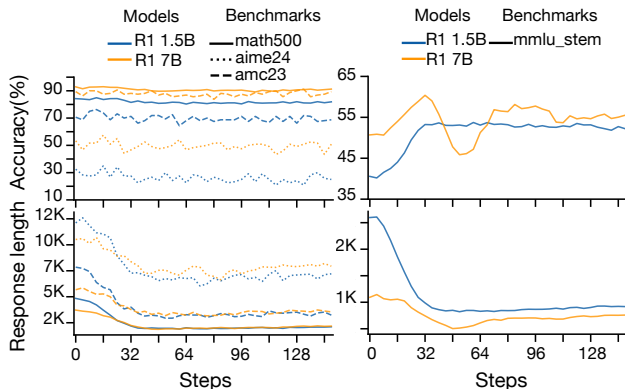


Figure 4: Response dynamics of two base models, **R1-1.5B** and **R1-7B**. Both models are trained with PPO using 8 problems from the level-5 subset of MATH dataset. **Left:** three mathematics benchmarks (different line styles). **Right:** STEM subset of the MMLU dataset. Response length and accuracy are shown against training checkpoints (steps). Response length decreased significantly, while accuracy remained stable or improved across benchmarks and model sizes.

Table 2 summarizes model performance on 8 problems from the MATH training subset, along with their base models. Checkpoints were selected to minimize response length while maintaining reasonable accuracy. Further analysis is needed to identify the optimal balance, as some checkpoints offer higher accuracy and others shorter responses, allowing for trade-offs based on given priorities.

Table 2: Comparison of R1 1.5B and R1 7B, and their post-trained versions on various benchmarks.

Benchmarks	R1 1.5B				R1 7B			
	Accuracy (%)		Length (tokens)		Accuracy (%)		Length (tokens)	
	Baseline	Ours	Baseline	Ours	Baseline	Ours	Baseline	Ours
math500 (500)	84.2	81.0	4842	1965	92.9	90.3	3718	2041
aime24 (30)	32.5	30.0	12104	6752	53.3	51.7	10510	6632
amc23 (40)	70.6	69.4	7847	2936	89.4	88.1	5674	3220
mmlu_stem (3018)	40.6	53.1	2597	821	50.7	58.1	1093	701
average	57.0	58.4	6848	3119	71.6	72.1	5249	3149

7.3 Increase in Performance and Robustness

In the previous section, we showed that further RL post training results in response length reduction while maintaining accuracy. In this section, we provide evidence that further RL post training also improves the model in terms of robustness and performance.

To assess model robustness, we examine their sensitivity to temperature settings. Setting the temperature to zero can severely degrade the accuracy of reasoning models like R1. However, standard metrics such as pass@1, which rely on multiple samples at non-zero temperatures, often obscure the benefits of secondary RL post-training on a small dataset.

We experimented with temperature 0 and 0.6 and observed that when the temperature was set to zero, the post trained model significantly outperformed the baseline model, suggesting the robustness of the post trained model compared to the base model (see Table 3).

Table 3: Performance degrade of reasoning models with temperature.

	Base Model		Ours	
	MATH500	AIME24	MATH500	AIME24
temperature=0, n=1	70%	13.3%	81%	23.3%
temperature=0.6, n=4	84.3%	32.5%	81%	30%
Relative Degrade	16.9%	59%	0%	22.3%

We also show that further RL training on a limited number of examples can result in a significant improvement in accuracy. This effect depends on the extent of prior RL training on similar (or even the same) problems. If a model has already undergone extensive RL-based training, further gains in accuracy may be more challenging to achieve.

To investigate this, we applied online RL to Qwen-Math-v2.5 on 4 examples from the MATH dataset. Unlike R1, this model has been trained on a large corpus of mathematical data solely through token completion as opposed to RL training. As shown in Table 4, we observed a surprisingly large improvement—up to 30% in the 1.5B model—demonstrating that RL post-training on only 4 problems can yield substantial accuracy gains, particularly in models that have not previously undergone RL-based reasoning refinement.

Table 4: Comparison of the baseline model and the RL-trained model using 4 examples (ours) across different base models and benchmarks shows a substantial accuracy gain with RL training.

Model	MATH500		AIME24		AMC23	
	Baseline	Ours	Baseline	Ours	Baseline	Ours
Qwen2.5-Math-7B	47.45	67.05	15.83	23.33	43.75	57.50
Qwen2.5-Math-1.5B	33.45	63.05	6.67	9.17	30.00	48.12
Qwen2.5-7B	54.30	70.20	5.00	10.83	40.00	54.38

8 Related Work

Recent large language models (LLMs) have been fine-tuned with reinforcement learning (RL) to enhance complex reasoning abilities. OpenAI’s *o1* model was among the first to use large-scale RL to encourage chain-of-thought (CoT) reasoning, leading to significant gains on challenging math and coding benchmarks. DeepSeek-R1 demonstrated that pure RL post-training (without supervised warm-up) can directly induce strong reasoning capabilities in LLMs. The model exhibited emergent behaviors like self-verification and multi-step planning, and achieved performance competitive with *o1*. Similarly, the Kimi k1.5 project scaled RL-based training with extremely long context windows and efficient PPO fine-tuning, enabling the model to backtrack and self-correct [18]. These models underscore the growing importance of RL for enhancing reasoning capabilities.

Beyond large proprietary models, several open research efforts have applied RL to improve reasoning. [19] proposed DialCoT-PPO, which transforms problem solving into a dialogue-based reasoning chain and trains the model to optimize these steps. Reinforced Fine-Tuning (ReFT) has been introduced, combining supervised warm-up with PPO-based exploration of diverse reasoning trajectories, significantly improving accuracy on GSM8K, MathQA, and SVAMP [20]. Self-Explore was introduced, where the model identifies and learns from its own mistakes in reasoning paths [21]. These works demonstrate the versatility of RL in refining reasoning processes across various tasks and model sizes.

While it is commonly assumed that longer responses inherently lead to better reasoning accuracy, empirical findings are mixed. On one hand, increased response length has been associated with improved accuracy [2–4]. It has shown that a collapse in response length can lead to a degradation in performance [22]. Reward shaping techniques have been employed to encourage longer outputs [23]. On the other hand, several works have found that longer responses do not necessarily correlate with better performance [4, 24], and reported diminishing returns—and even performance degradation—when responses became excessively long Wu et al. [25]. Our work provides a deeper understanding of the relationship between response length and accuracy, offering new insights into how these two factors are correlated.

Moreover, while long reasoning traces may improve accuracy, they also increase token usage and latency. Recent studies have applied prompting strategies to limit chain of thoughts and analyzed the resulting impact on accuracy [26–30]. It has been shown that each problem has an intrinsic “token complexity”: reducing token count below this threshold significantly harms performance. Current prompt-based strategies for conciseness (e.g., “think step by step, but briefly”) often fall short of this optimal limit, revealing opportunities for improvement in efficient reasoning [31].

To improve efficiency, researchers have explored smaller or faster models (e.g., OpenAI’s *o1-mini*) and reward shaping during training. A cosine length-scaling reward has been proposed to promote productive CoT reasoning without verbosity [3]. Others explored long-to-short distillation—training with verbose CoTs for accuracy, then compressing reasoning via model merging or shortest-path sampling. The Kimi team showed that these compressed reasoning models can outperform even GPT-4 on some tasks while using fewer tokens. Our work suggests that a second phase of RL training can substantially shorten response lengths while maintaining accuracy.

9 Concluding Remarks

In this paper, we provided a more comprehensive view of how response length interacts with performance in reasoning models. We proposed a two-phase RL post-training strategy to first improve reasoning in the base model followed by enforcing conciseness. Our methodology substantially improved R1 models by achieving **over 54% and 40% reduction in response length for the R1 1.5B and R1 7B models**, respectively, while preserving accuracy and delivering significantly improved performance at low temperatures. Our analysis and empirical findings lead to several key takeaways that may be useful to practitioners:

1. Substantial improvements can be achieved for non-reasoning models through minimal RL training.
2. Response conciseness can be enhanced without compromising accuracy.
3. In PPO training, setting $\lambda < 1$ is critical for robustness.
4. Training data should adequately include problems that are occasionally solvable to ensure conciseness reinforcement.
5. GRPO can achieve faster training than PPO, but it becomes unstable as more problems are solved.
6. To enhance both accuracy and conciseness, RL training can be structured in two phases. The first phase prioritizes accuracy and generalization, even if it results in prolixity. The second phase focuses on conciseness while preserving the accuracy established in the first phase.

Data and Code Availability

Our code to replicate the analysis (including figures) presented in this paper is available at <https://github.com/ai-wand/concise-reasoning>.

Acknowledgment

The authors would like to thank Hyun Ahn for the insightful feedback on the early version of this paper. Special thanks are also extended to the Fundamental Research team at Wand AI for the valuable and stimulating discussions.

References

- [1] Richard S. Sutton and Andrew G. Barto. *Reinforcement Learning: An Introduction*. The MIT Press, second edition, 2018. URL <http://incompleteideas.net/book/the-book-2nd.html>.
- [2] Daya Guo, Dejian Yang, Haowei Zhang, Junxiao Song, Ruoyu Zhang, Runxin Xu, Qihao Zhu, Shirong Ma, Peiyi Wang, Xiao Bi, et al. Deepseek-rl: Incentivizing reasoning capability in llms via reinforcement learning. *arXiv preprint arXiv:2501.12948*, 2025.
- [3] Edward Yeo, Yuxuan Tong, Morry Niu, Graham Neubig, and Xiang Yue. Demystifying long chain-of-thought reasoning in llms, 2025. URL <https://arxiv.org/abs/2502.03373>.
- [4] Weihao Zeng, Yuzhen Huang, Qian Liu, Wei Liu, Keqing He, Zejun Ma, and Junxian He. Simplerl-zoo: Investigating and taming zero reinforcement learning for open base models in the wild. *arXiv preprint arXiv:2503.18892*, 2025.
- [5] Jiayi Pan, Junjie Zhang, Xingyao Wang, Lifan Yuan, Hao Peng, and Alane Suhr. Tinyzero. <https://github.com/Jiayi-Pan/TinyZero>, 2025. Accessed: 2025-01-24.
- [6] Michael Luo, Sijun Tan, Justin Wong, Xiaoxiang Shi, William Y. Tang, Manan Roongta, Colin Cai, Jeffrey Luo, Tianjun Zhang, Li Erran Li, Raluca Ada Popa, and Ion Stoica. Deepscaler: Surpassing o1-preview with a 1.5b model by scaling rl, 2025. Notion Blog.
- [7] Mehdi Fatemi, Shikhar Sharma, Harm Van Seijen, and Samira Ebrahimi Kahou. Dead-ends and secure exploration in reinforcement learning. In Kamalika Chaudhuri and Ruslan Salakhutdinov, editors, *Proceedings of the 36th International Conference on Machine Learning*, volume 97 of *Proceedings of Machine Learning Research*, pages 1873–1881, Long Beach, California, USA, 2019. PMLR.
- [8] Mehdi Fatemi, Taylor W Killian, Jayakumar Subramanian, and Marzyeh Ghassemi. Medical dead-ends and learning to identify high-risk states and treatments. In M Ranzato, A Beygelzimer, Y Dauphin, P S Liang, and J Wortman Vaughan, editors, *Advances in Neural Information Processing Systems*, volume 34, pages 4856–4870. Curran Associates, Inc., 2021.
- [9] Meng Cao, Mehdi Fatemi, Jackie C K Cheung, and Samira Shabanian. Systematic rectification of language models via dead-end analysis. In *The Eleventh International Conference on Learning Representations*, 2023.
- [10] Martin L Puterman. *Markov decision processes: discrete stochastic dynamic programming*. John Wiley & Sons, 2014.
- [11] John Schulman, Filip Wolski, Prafulla Dhariwal, Alec Radford, and Oleg Klimov. Proximal policy optimization algorithms, 2017. URL <http://arxiv.org/abs/1707.06347>. cite arxiv:1707.06347.
- [12] Chaoqun He, Renjie Luo, Yuzhuo Bai, Shengding Hu, Zhen Leng Thai, Junhao Shen, Jinyi Hu, Xu Han, Yujie Huang, Yuxiang Zhang, Jie Liu, Lei Qi, Zhiyuan Liu, and Maosong Sun. Olympiadbench: A challenging benchmark for promoting agi with olympiad-level bilingual multimodal scientific problems, 2024.
- [13] John Schulman, Philipp Moritz, Sergey Levine, Michael I. Jordan, and Pieter Abbeel. High-dimensional continuous control using generalized advantage estimation. In Yoshua Bengio and Yann LeCun, editors, *4th International Conference on Learning Representations, ICLR 2016, San Juan, Puerto Rico, May 2-4, 2016, Conference Track Proceedings*, 2016.
- [14] Dimitri P. Bertsekas and John N. Tsitsiklis. *Neuro-Dynamic Programming*. Athena Scientific, 1996.
- [15] Zhihong Shao, Peiyi Wang, Qihao Zhu, Runxin Xu, Junxiao Song, Xiao Bi, Haowei Zhang, Mingchuan Zhang, Y. K. Li, Y. Wu, and Daya Guo. Deepseekmath: Pushing the limits of mathematical reasoning in open language models, 2024.

- [16] Zichen Liu, Changyu Chen, Wenjun Li, Penghui Qi, Tianyu Pang, Chao Du, Wee Sun Lee, and Min Lin. Understanding r1-zero-like training: A critical perspective, 2025. URL <https://arxiv.org/abs/2503.20783>.
- [17] Dan Hendrycks, Collin Burns, Saurav Kadavath, Akul Arora, Steven Basart, Eric Tang, Dawn Song, and Jacob Steinhardt. Measuring mathematical problem solving with the math dataset. *arXiv preprint arXiv:2103.03874*, 2021.
- [18] Kimi Team, Angang Du, Bofei Gao, Bowei Xing, Changjiu Jiang, Cheng Chen, Cheng Li, Chenjun Xiao, Chenzhuang Du, Chonghua Liao, et al. Kimi k1. 5: Scaling reinforcement learning with llms. *arXiv preprint arXiv:2501.12599*, 2025.
- [19] Chengcheng Han, Xiaowei Du, Che Zhang, Yixin Lian, Xiang Li, Ming Gao, and Baoyuan Wang. Dialcot meets ppo: Decomposing and exploring reasoning paths in smaller language models. *arXiv preprint arXiv:2310.05074*, 2023.
- [20] Trung Quoc Luong, Xinbo Zhang, Zhanming Jie, Peng Sun, Xiaoran Jin, and Hang Li. Reft: Reasoning with reinforced fine-tuning. *arXiv preprint arXiv:2401.08967*, 2024.
- [21] Hyeonbin Hwang, Doyoung Kim, Seungone Kim, Seonghyeon Ye, and Minjoon Seo. Self-explore: Enhancing mathematical reasoning in language models with fine-grained rewards. *arXiv preprint arXiv:2404.10346*, 2024.
- [22] Yufeng Yuan, Yu Yue, Ruofei Zhu, Tiantian Fan, and Lin Yan. What’s behind ppo’s collapse in long-cot? value optimization holds the secret. *arXiv preprint arXiv:2503.01491*, 2025.
- [23] Guanghao Ye, Khiem Duc Pham, Xinzhi Zhang, Sivakanth Gopi, Baolin Peng, Beibin Li, Janardhan Kulkarni, and Huseyin A Inan. On the emergence of thinking in llms i: Searching for the right intuition. *arXiv preprint arXiv:2502.06773*, 2025.
- [24] Tian Xie, Zitian Gao, Qingnan Ren, Haoming Luo, Yuqian Hong, Bryan Dai, Joey Zhou, Kai Qiu, Zhirong Wu, and Chong Luo. Logic-r1: Unleashing llm reasoning with rule-based reinforcement learning. *arXiv preprint arXiv:2502.14768*, 2025.
- [25] Yuyang Wu, Yifei Wang, Tianqi Du, Stefanie Jegelka, and Yisen Wang. When more is less: Understanding chain-of-thought length in llms. *arXiv preprint arXiv:2502.07266*, 2025.
- [26] Silei Xu, Wenhao Xie, Lingxiao Zhao, and Pengcheng He. Chain of draft: Thinking faster by writing less. *arXiv preprint arXiv:2502.18600*, 2025.
- [27] Matthew Renze and Erhan Guven. The benefits of a concise chain of thought on problem-solving in large language models. In *2024 2nd International Conference on Foundation and Large Language Models (FLLM)*, pages 476–483. IEEE, 2024.
- [28] Mingyu Jin, Qinkai Yu, Dong Shu, Haiyan Zhao, Wenyue Hua, Yanda Meng, Yongfeng Zhang, and Mengnan Du. The impact of reasoning step length on large language models. *arXiv preprint arXiv:2401.04925*, 2024.
- [29] Sania Nayab, Giulio Rossolini, Marco Simoni, Andrea Saracino, Giorgio Buttazzo, Nicolamaria Manes, and Fabrizio Giacomelli. Concise thoughts: Impact of output length on llm reasoning and cost. *arXiv preprint arXiv:2407.19825*, 2024.
- [30] Niklas Muennighoff, Zitong Yang, Weijia Shi, Xiang Lisa Li, Li Fei-Fei, Hannaneh Hajishirzi, Luke Zettlemoyer, Percy Liang, Emmanuel Candès, and Tatsunori Hashimoto. s1: Simple test-time scaling. *arXiv preprint arXiv:2501.19393*, 2025.
- [31] Ayeong Lee, Ethan Che, and Tianyi Peng. How well do llms compress their own chain-of-thought? a token complexity approach. *arXiv preprint arXiv:2503.01141*, 2025.

A Appendix

A.1 Applying Penalty and Discounting

Although RL training on a small number of sufficiently difficult problems naturally encourages more concise responses, this effect can be further reinforced by introducing an explicit incentive for brevity. In RL, there are two primary methods to promote shorter responses: discounting the return and applying a negative reward per step (or per excessive token use). While both approaches have limitations, the drawbacks of negative rewards are particularly severe. Introducing a step-wise penalty can create strong local optima that hinder effective learning. For instance, the model might prematurely terminate its response to minimize the cumulative penalty rather than fully solving the problem. Moreover, for negative rewards to meaningfully influence learning, they must be large enough to affect decision-making, yet not so dominant that their accumulation overshadows the positive reward of reaching a correct answer. Given that different problems require varying response lengths, finding an optimal penalty value that works across all cases can be impractical.

Using a discount factor mitigates these issues, as it avoids altering the model’s fundamental reasoning process and does not introduce misleading local optima. However, as discussed in Section 4, it inherently introduces an incremental difference between the value of the subsequent steps. This can dilute the return more than expected and effectively shortens the agent’s decision horizon, meaning that distant rewards become less influential. If the required chain of thought extends beyond this effective horizon, the agent may fail to recognize the value of a correct answer, leading to potential accuracy degradation. The extent of this adverse effect depends on the chosen discount factor. We therefore recommend to use λ to avoid these complications while benefiting the impact, as explained in Section 4.

A.2 Value Behaviour of PPO

Due to random initialization, the initial value network produces values near zero. At each training step, the KL penalty encourages alignment with the value network of the previous step. As the value training continues, V gradually moves from zero toward G . Consequently, the KL penalty drives V toward zero to maintain similarity to the old values, whereas the regression loss pushes it toward G . This opposition creates an equilibrium point between zero and G where the two losses balance each other. If the KL weight is small, this equilibrium point will be close to G . When V exceeds G , both losses align, pulling V toward zero and quickly restoring equilibrium. Consequently, when $G > 0$, the value will almost surely *underestimate* it, whereas when $G < 0$, the value will almost surely *overestimate* it. The amount of this under/overestimation depend directly on the KL weight.

A.3 Problems from OlympiadBench and AIME Used for Training

For the experiment on OlympiadBench, we used problems from the Hugging Face dataset Hothan/OlympiadBench with IDs 2231,2237,2240,2245. For the experiments on the AIME24 dataset, we used 4 sets of training examples from the Hugging Face dataset HuggingFaceH4/aime_2024. The set with $\bar{p}_a = 0.16$ included problems with IDs 65, 82, 83, 76. The set with $\bar{p}_a = 0.25$ included problems with IDs 65, 64, 61, 76. The set with $\bar{p}_a = 0.375$ included problems with IDs 61, 64, 71, 74. Finally, the fourth set included problems with IDs 71, 74, 82, 86.

A.4 Advantage Behaviour of a Group in GRPO

Let x_1, x_2, \dots, x_N be a set of N binary samples where each $x_i \in \{0, 1\}$. Denote by k the number of ones in the set, so the empirical mean is

$$\mu = \frac{1}{N} \sum_{i=1}^N x_i = \frac{k}{N}.$$

The population variance is given by

$$\sigma^2 = \frac{1}{N} \sum_{i=1}^N (x_i - \mu)^2 = \mu(1 - \mu) = \frac{k}{N} \left(1 - \frac{k}{N}\right),$$

and thus the standard deviation is

$$\sigma = \sqrt{\frac{k}{N} \left(1 - \frac{k}{N}\right)}.$$

We now analyze the range of possible values for σ .

Minimum. The standard deviation is minimized when all samples are identical, i.e., when $k = 0$ or $k = N$. In either case, $\mu \in \{0, 1\}$, and we have

$$\sigma = \sqrt{\mu(1 - \mu)} = 0.$$

Maximum. The function $f(p) = p(1 - p)$ achieves its maximum at $p = \frac{1}{2}$, yielding

$$\sigma = \sqrt{\frac{1}{2} \left(1 - \frac{1}{2}\right)} = \frac{1}{2}.$$

This maximum is achieved when $k = \frac{N}{2}$, which is possible only if N is even. For odd N , the maximum is attained at $k = \lfloor N/2 \rfloor$ or $k = \lceil N/2 \rceil$, in which case the standard deviation is slightly less than $\frac{1}{2}$:

$$\sigma = \sqrt{\frac{k}{N} \left(1 - \frac{k}{N}\right)}, \quad \text{where } k = \left\lfloor \frac{N}{2} \right\rfloor \text{ or } \left\lceil \frac{N}{2} \right\rceil.$$

Hence, for any set of N binary samples:

$$0 \leq \sigma \leq \frac{1}{2},$$

with the minimum attained when all samples are identical, and the maximum attained when the number of ones and zeros is (nearly) equal.

Standard Deviation for $k = 1$ and Various N .

$$\sigma = \sqrt{\frac{1}{N} \left(1 - \frac{1}{N}\right)} = \sqrt{\frac{N-1}{N^2}},$$

we compute the standard deviation for different values of N :

- For $N = 8$: $\sigma = \sqrt{\frac{7}{64}} \approx 0.3307$
- For $N = 16$: $\sigma = \sqrt{\frac{15}{256}} \approx 0.2425$
- For $N = 64$: $\sigma = \sqrt{\frac{63}{4096}} \approx 0.1242$
- For $N = 256$: $\sigma = \sqrt{\frac{255}{65536}} \approx 0.0622$

Exactly the same results for $k = N - 1$ and various N since

$$\sigma = \sqrt{\frac{N-1}{N} \left(1 - \frac{N-1}{N}\right)} = \sqrt{\frac{N-1}{N^2}},$$

Using σ and μ , we can directly compute \hat{A} in a closed form as follows

- If $r = 1$:

$$\frac{1 - \mu}{\sigma} = \frac{1 - \frac{k}{N}}{\sqrt{\frac{k(N-k)}{N^2}}} = \frac{N-k}{\sqrt{k(N-k)}} = \sqrt{\frac{N-k}{k}}.$$

- If $r = 0$:

$$\frac{0 - \mu}{\sigma} = \frac{-\frac{k}{N}}{\sqrt{\frac{k(N-k)}{N^2}}} = -\frac{k}{\sqrt{k(N-k)}} = -\sqrt{\frac{k}{N-k}}.$$

Thus,

$$\hat{A} = \frac{r - \mu}{\sigma} = \begin{cases} \sqrt{\frac{N-k}{k}}, & \text{if } r = 1 \\ -\sqrt{\frac{k}{N-k}}, & \text{if } r = 0 \end{cases}$$

Table 5 shows \hat{A} for various values of N and k .

Conclusion. Based on the numbers above, we can conclude that in the case of Dr.GRPO [16], omitting the division by σ **decreases** the advantage, and thus the loss, by nearly a factor of 3 for a group size of 8, and by up to 10 times for group sizes between 64 and 128. However, removing response length from the denominator leads to a substantial **increase** in loss magnitude, ranging from about 1K to 30K, which is far larger than the diminish from removing σ .

N	k	$\frac{r-\mu}{\sigma}$ for $r = 1$	$\frac{r-\mu}{\sigma}$ for $r = 0$
8	1	2.6458	-0.3780
	2	1.7321	-0.5774
	3	1.2910	-0.7746
	5	0.7746	-1.2910
	6	0.5774	-1.7321
	7	0.3780	-2.6458
	16	1	3.8730
2		2.6458	-0.3780
3		2.0801	-0.4961
13		0.4961	-2.0801
14		0.3780	-2.6458
15		0.2582	-3.8730
64	1	7.9373	-0.1260
	2	5.5902	-0.1796
	3	4.5255	-0.2182
	61	0.2182	-4.5255
	62	0.1796	-5.5902
	63	0.1260	-7.9373
256	1	15.9687	-0.0626
	2	11.2900	-0.0886
	3	9.2085	-0.1086
	253	0.1086	-9.2085
	254	0.0886	-11.2900
	255	0.0626	-15.9687

Table 5: Values of $\hat{A} = \frac{r-\mu}{\sigma}$ for binary samples, across various values of N and k . The sign indicates whether the sample is above or below the mean.

A.5 Proofs

A.5.1 Theorem 1 — PPO Loss under GAE

The total advantage sum can be expanded as

$$\sum_{t=0}^{T-1} \hat{A}_t = \sum_{t=0}^{T-1} \sum_{l=0}^{T-t-1} \lambda^l \delta_{t+l} = \sum_{k=0}^{T-1} \delta_k \sum_{t=0}^k \lambda^{k-t} = \sum_{k=0}^{T-1} \delta_k \sum_{j=0}^k \lambda^j \quad (4)$$

The second equality is obtained by setting $k = t + l$ and then swapping the summations ($0 \leq t \leq k \leq T - 1$). We define the GAE weight for each δ_k and rewrite the total advantage as the following:

$$w_k := \sum_{j=0}^k \lambda^j \geq 0, \quad \sum_{t=0}^{T-1} \hat{A}_t = \sum_{k=0}^{T-1} w_k \delta_k$$

Let us separate the last token from the rest,

- For $k \in \{0, \dots, T - 2\}$, $\delta_k = V(s_{k+1}) - V(s_k)$, and $|\delta_k| \leq \epsilon$, we have

$$-\epsilon \sum_{k=0}^{T-2} w_k \leq \sum_{k=0}^{T-2} w_k \delta_k \leq \epsilon \sum_{k=0}^{T-2} w_k$$

- For the last token, $k = T - 1$, we have $\delta_{T-1} = r + V(s_T) - V(s_{T-1})$.

By definition, $V(s_T) = 0$. We define $R := \delta_{T-1} = r - V(s_{T-1})$. In Appendix A.2 we have shown that when $r > 0$, V underestimates and when $r < 0$, V overestimates. Thus, R has the same sign as r . We write

$$\sum_{t=0}^{T-1} \hat{A}_t = R \cdot w_{T-1} + E \quad \text{with} \quad |E| \leq \epsilon \sum_{k=0}^{T-2} w_k$$

E is the total value-estimate error before the last token. Average PPO loss is then reduced to

$$L_{\text{avg}} \propto -\frac{1}{T} (R \cdot w_{T-1} + E) \quad (5)$$

First, let us consider the case of $\lambda < 1$. We can write w_k as

$$w_k = \sum_{j=0}^k \lambda^j = \frac{1 - \lambda^{k+1}}{1 - \lambda}$$

For large T , we have

$$w_{T-1} = \frac{1 - \lambda^T}{1 - \lambda} \rightarrow \frac{1}{1 - \lambda}, \quad \sum_{k=0}^{T-2} w_k \rightarrow \sum_{k=0}^{T-2} \frac{1}{1 - \lambda} = \frac{T-1}{1 - \lambda} < \frac{T}{1 - \lambda}$$

Therefore we write

$$\frac{\epsilon}{T} \sum_{k=0}^{T-2} w_k \leq \frac{\epsilon}{T} \cdot \frac{T}{1 - \lambda} = \frac{\epsilon}{1 - \lambda}$$

Thus, from (5), the total average loss becomes

$$L_{\text{avg}} \propto -\frac{R}{T(1 - \lambda)} + O\left(\frac{\epsilon}{1 - \lambda}\right) \quad (6)$$

For the case of $\lambda = 1$, we have $w_k = \sum_{j=0}^k 1^j = k + 1$, and $\sum_{k=0}^{T-2} (k + 1) = \frac{(T-1)T}{2}$. Thus, $|E| \leq \epsilon \frac{T(T-1)}{2}$, and we write

$$L_{\text{avg}} \propto -R + O\left(\frac{\epsilon \cdot T}{2}\right) \quad (7)$$

A.5.2 Theorem 2 — GRPO Prolixity

Since $\hat{A}_t^{(i)} = \hat{A}^{(i)}$, we rewrite (1) as

$$L_{\text{GRPO}}(\pi_\theta) = \begin{cases} -\mathbb{E}_{q \sim p_Q, \{o^{(i)}\}_{i=0}^{G-1} \sim \pi_{\theta_{\text{old}}}} \left[\frac{1}{G} \sum_{i=0}^{G-1} \frac{\hat{A}_i}{|o^{(i)}|} \sum_{t=0}^{|o^{(i)}|-1} \min \left(\frac{\pi_\theta(o_t^{(i)} | q, o_{<t}^{(i)})}{\pi_{\theta_{\text{old}}}(o_t^{(i)} | q, o_{<t}^{(i)})}, 1 + \epsilon \right) \right], & \text{if } \hat{A}_i > 0 \\ -\mathbb{E}_{q \sim p_Q, \{o^{(i)}\}_{i=0}^{G-1} \sim \pi_{\theta_{\text{old}}}} \left[\frac{1}{G} \sum_{i=0}^{G-1} \frac{\hat{A}_i}{|o^{(i)}|} \sum_{t=0}^{|o^{(i)}|-1} \max \left(\frac{\pi_\theta(o_t^{(i)} | q, o_{<t}^{(i)})}{\pi_{\theta_{\text{old}}}(o_t^{(i)} | q, o_{<t}^{(i)})}, 1 - \epsilon \right) \right], & \text{if } \hat{A}_i < 0 \end{cases}$$

Without loss of generality, consider a fixed group and focus on a single response with length T within the group. We examine how the loss behaves under two scenarios: in the first, the policy assigns a high probability of terminating the response at token $T - 1$; in the second, it assigns a low probability of terminating at $T - 1$ but instead continues with one additional token, terminating at token T , with a probability comparable to the first scenario's stopping probability at $T - 1$. The goal is to understand how the loss changes under these two behaviors, depending on whether the advantage is positive or negative.

Since the group is fixed, we only need to consider the contribution of this sample in the loss; we call it L . To simplify the notation, for the chosen response, define o_t as the t -th token. The theorem only concern token $T - 1$ and how it impacts the loss. Hence, by construction, all tokens up to and including $T - 2$ are **fixed** and the expectation only affects token $T - 1$. With notation simplifications, it therefore deduces

$$L(\pi_\theta) = \begin{cases} -\frac{\hat{A}}{T} \mathbb{E}_{o_{T-1} \sim \pi_{\theta_{\text{old}}}} \left[\sum_{t=0}^{T-1} \min \left(\frac{\pi_\theta(o_t)}{\pi_{\theta_{\text{old}}}(o_t)}, 1 + \epsilon \right) \right], & \text{if } \hat{A} > 0 \\ -\frac{\hat{A}}{T} \mathbb{E}_{o_{T-1} \sim \pi_{\theta_{\text{old}}}} \left[\sum_{t=0}^{T-1} \max \left(\frac{\pi_\theta(o_t)}{\pi_{\theta_{\text{old}}}(o_t)}, 1 - \epsilon \right) \right], & \text{if } \hat{A} < 0 \end{cases}$$

where \hat{A} is the advantage of the selected response. Separating the first $T - 1$ fixed tokens, it yields

$$L(\pi_\theta) = \begin{cases} -\frac{\hat{A}}{T} \sum_{t=0}^{T-2} \min \left(\frac{\pi_\theta(o_t)}{\pi_{\theta_{\text{old}}}(o_t)}, 1 + \epsilon \right) - \frac{\hat{A}}{T} \mathbb{E}_{o_{T-1} \sim \pi_{\theta_{\text{old}}}} \min \left(\frac{\pi_\theta(o_{T-1})}{\pi_{\theta_{\text{old}}}(o_{T-1})}, 1 + \epsilon \right), & \text{if } \hat{A} > 0 \\ -\frac{\hat{A}}{T} \sum_{t=0}^{T-2} \max \left(\frac{\pi_\theta(o_t)}{\pi_{\theta_{\text{old}}}(o_t)}, 1 - \epsilon \right) - \frac{\hat{A}}{T} \mathbb{E}_{o_{T-1} \sim \pi_{\theta_{\text{old}}}} \max \left(\frac{\pi_\theta(o_{T-1})}{\pi_{\theta_{\text{old}}}(o_{T-1})}, 1 - \epsilon \right), & \text{if } \hat{A} < 0 \end{cases}$$

$$= \begin{cases} -\frac{\hat{A}}{T} \beta_1 - \frac{\hat{A}}{T} \mathbb{E}_{o_{T-1} \sim \pi_{\theta_{\text{old}}}} \min \left(\frac{\pi_\theta(o_{T-1})}{\pi_{\theta_{\text{old}}}(o_{T-1})}, 1 + \epsilon \right), & \text{if } \hat{A} > 0 \\ -\frac{\hat{A}}{T} \beta_2 - \frac{\hat{A}}{T} \mathbb{E}_{o_{T-1} \sim \pi_{\theta_{\text{old}}}} \max \left(\frac{\pi_\theta(o_{T-1})}{\pi_{\theta_{\text{old}}}(o_{T-1})}, 1 - \epsilon \right), & \text{if } \hat{A} < 0 \end{cases} \quad (8)$$

where $\beta_1 > 0$ and $\beta_2 > 0$ are the first terms of the two equations, respectively. By assumption, π_θ and $\pi_{\theta_{\text{old}}}$ are identical for $t \leq T - 2$. Hence, $\beta_1 = \beta_2 = B = T - 1$. Note that in general $0 < \beta_1 \leq (T - 1)(1 + \epsilon)$ and $\beta_2 \geq (T - 1)(1 - \epsilon)$. However, even in the general case, the KL regularization should naturally keep most sampling ratios close to one, meaning that both β s should remain close to $T - 1$.

Recall that the response is sampled from $\pi_{\theta_{\text{old}}}$. Let τ denote the terminal token. Assume that $\pi_{\theta_{\text{old}}}(o_{T-1} = \tau) \neq 0$, and that this probability is neither too small nor too large. Let a trajectory sampled from $\pi_{\theta_{\text{old}}}$ produce a sequence of length T , meaning $o_{T-1} = \tau$. We consider a new policy π_θ that matches $\pi_{\theta_{\text{old}}}$ exactly for all $t \leq T - 2$, differing only at the final token. Our objective is to analyze how modifying π_θ in this way affects the loss, under the conditions $\hat{A} > 0$ and $\hat{A} < 0$.

Case 1 ($\hat{A} > 0$): If $\pi_\theta(o_{T-1} = \tau)$ decreases relative to $\pi_{\theta_{\text{old}}}(o_{T-1} = \tau)$, then the ratio $\frac{\pi_\theta}{\pi_{\theta_{\text{old}}}}$ becomes smaller, which is favored by the min operator in Equation (8). Consequently, the loss increases (becomes less negative). Conversely, if $\pi_\theta(o_{T-1} = \tau)$ increases, the loss decreases (up to $1 + \epsilon$). Therefore, when $\hat{A} > 0$, GRPO encourages raising $\pi_\theta(o_{T-1} = \tau)$, effectively increasing the probability of termination and discouraging longer sequences.

Case 2 ($\hat{A} < 0$): If $\pi_\theta(o_{T-1} = \tau)$ increases relative to $\pi_{\theta_{\text{old}}}(o_{T-1} = \tau)$, then the ratio $\frac{\pi_\theta}{\pi_{\theta_{\text{old}}}}$ can grow unboundedly, which is favored by the max operator in Equation (8). Since $-\hat{A} > 0$, this results

in an increase in the loss. Conversely, if $\pi_\theta(o_{T-1} = \tau)$ decreases, the loss is reduced, down to $1 - \epsilon$. Therefore, when $\hat{A} < 0$, GRPO encourages reducing $\pi_\theta(o_{T-1} = \tau)$, effectively lowering the probability of termination and promoting longer sequences.

A.5.3 Theorem 3 — General Conciseness

Let π_θ be a parameterized stochastic policy, and $\pi_{\theta_{\text{old}}}$ be the policy before the update. If the advantage estimate for response i is positive, i.e., $\hat{A}^{(i)} > 0$, both PPO and GRPO optimize a clipped surrogate objective:

$$L^{(i)}(\theta) = -\hat{A}^{(i)} \cdot \frac{1}{T_i} \sum_{t=0}^{T_i-1} \min\left(\rho_t^{(i)}, 1 + \epsilon\right), \quad \rho_t^{(i)} = \frac{\pi_\theta(o_t^{(i)} | o_{<t}^{(i)})}{\pi_{\theta_{\text{old}}}(o_t^{(i)} | o_{<t}^{(i)})},$$

where T_i is the length of response i , and $\epsilon > 0$ is a clipping threshold. This loss term then contributes to the total average loss, which is minimized by the optimizer.

The loss is a function of π_θ , but the trajectories are sampled from π_{old} , which is fixed during optimization. Therefore, the gradient is computed with respect to the numerator of $\rho_t^{(i)}$, treating π_{old} as a constant (for clarity, we drop all the conditioning in the policies):

$$\nabla_\theta \rho_t^{(i)} = \nabla_\theta \left(\frac{\pi_\theta(o_t^{(i)})}{\pi_{\theta_{\text{old}}}(o_t^{(i)})} \right) = \frac{1}{\pi_{\theta_{\text{old}}}(o_t^{(i)})} \nabla_\theta \pi_\theta(o_t^{(i)}) = \rho_t^{(i)} \nabla_\theta \log \pi_\theta(o_t^{(i)}) \quad (9)$$

We break the loss into per-tokens, $L^{(i)} = \sum_{t=0}^{T-1} L_t^{(i)}$. Therefore, for token t we write

$$\nabla_\theta L_t^{(i)} = -\hat{A}^{(i)} \cdot \frac{1}{T_i} \nabla_\theta \min(\rho_t^{(i)}, 1 + \epsilon).$$

Importantly, this gradient characterizes how token t is selected after the update. If $\rho_t < 1 + \epsilon$, the min operator vanishes and equation (9) yields

$$\nabla_\theta L_t^{(i)} = -\hat{A}^{(i)} \cdot \frac{1}{T} \nabla_\theta \rho_t^{(i)} = -\hat{A}^{(i)} \cdot \frac{1}{T} \cdot \rho_t^{(i)} \nabla_\theta \log \pi_\theta(o_t^{(i)}) \quad (10)$$

Let us focus on a fixed position t of the sequence. Assume that the last layer of π_θ is a softmax over K tokens with logits $\mathbf{z}(\theta) \in \mathbb{R}^K$. The probability assigned to token k is:

$$\pi_\theta(o_t^{(i)} = k) = \frac{e^{z_k}}{\sum_{j=1}^K e^{z_j}}.$$

where $\pi_\theta(k)$ is a short-hand for $\pi_\theta(o_t^k | o_{<t}^k)$ for a fixed t . To compute the gradient of the log-probability, we write

$$\log \pi_\theta(o_t^{(i)} = k) = z_k - \log \left(\sum_{j=1}^K e^{z_j} \right),$$

Differentiating with respect to \mathbf{z} yields

$$\nabla_{\mathbf{z}} \log \pi_\theta(o_t^{(i)} = k) = \nabla_{\mathbf{z}} z_k - \nabla_{\mathbf{z}} \log \left(\sum_{j=1}^K e^{z_j} \right).$$

The first term is simply \mathbf{e}_k , the one-hot vector with 1 in position k . The second term is the gradient of the log-partition function, which equals the softmax vector,

$$\nabla_{\mathbf{z}} \log \left(\sum_{j=1}^K e^{z_j} \right) = \left(\frac{e^{z_1}}{\sum_j e^{z_j}}, \dots, \frac{e^{z_K}}{\sum_j e^{z_j}} \right) = \boldsymbol{\pi}_\theta.$$

So we get

$$\nabla_{\mathbf{z}} \log \pi_\theta(k) = \mathbf{e}_k - \boldsymbol{\pi}_\theta.$$

This gradient is a vector in \mathbb{R}^K , and its squared norm is

$$\|\nabla_z \log \pi_\theta(o_t^{(i)} = k)\|^2 = \sum_{j=1}^K \left(\delta_{jk} - \pi_\theta(o_t^{(i)} = j) \right)^2 = \left(1 - \pi_\theta(o_t^{(i)} = k) \right)^2 + \sum_{j \neq k} \pi_\theta(o_t^{(i)} = j)^2 \quad (11)$$

with δ_{jk} denoting the Kronecker delta function. Defining $f(k) := \|\nabla_z \log \pi_\theta(k)\|$, equation (11) proves part 1 of the theorem.

For the next part, let us focus on the loss of the **first token**. By assumption, clipping is inactive for the first tokens of both sequences (i.e., $\rho_0^{(S)}, \rho_0^{(L)} < 1 + \epsilon$). Thus, from (10), the gradient of the surrogate loss for token $o_0^{(i)}$ with respect to model parameters θ is:

$$\nabla_\theta L^{(i)}(o_0^{(i)}) = -\frac{\hat{A}}{T_i} \rho_0^{(i)} \nabla_\theta \log \pi_\theta(o_0^{(i)}).$$

Since the policy π_θ is computed via a softmax over logits $\mathbf{z}(\theta) \in \mathbb{R}^K$, the chain rule yields:

$$\nabla_\theta \log \pi_\theta(o_0^{(i)}) = \left(\frac{\partial \mathbf{z}}{\partial \theta} \right)^\top \nabla_z \log \pi_\theta(o_0^{(i)}).$$

Thus, the full gradient norm becomes

$$\left\| \nabla_\theta L^{(i)}(o_0^{(i)}) \right\| = \frac{\hat{A}}{T_i} \rho_0^{(i)} \left\| \left(\frac{\partial \mathbf{z}}{\partial \theta} \right)^\top \nabla_z \log \pi_\theta(o_0^{(i)}) \right\| \quad (12)$$

Now consider comparing $\left\| \nabla_\theta L^{(S)}(o_0^{(S)}) \right\|$ and $\left\| \nabla_\theta L^{(L)}(o_0^{(L)}) \right\|$. These gradients differ in two ways: the softmax log-prob gradients, and the Jacobians of the logits w.r.t. θ .

However, at the first token position ($t = 0$), both sequences share the same context (i.e., the empty prefix or prompt), so the network's hidden activations leading up to \mathbf{z} are identical. The only variation is the sampled token at $t = 0$, which does not affect the computation of z_0 . Therefore, we have:

$$\left(\frac{\partial \mathbf{z}}{\partial \theta} \right)^{(S)} = \left(\frac{\partial \mathbf{z}}{\partial \theta} \right)^{(L)} := \mathbf{J}$$

where we define $\mathbf{J} \in \mathbb{R}^{K \times N}$ to be the common Jacobian matrix with K representing the vocabulary size, as before, and N the dimensionality of the parameter space, with the corresponding parameter vector $\theta \in \mathbb{R}^N$.

From expression (12), this yields

$$\begin{aligned} & \left\| \nabla_\theta L^{(S)}(o_0^{(S)}) \right\| > \left\| \nabla_\theta L^{(L)}(o_0^{(L)}) \right\| \\ \iff & \frac{\hat{A}}{T_S} \rho_0^{(S)} \left\| \mathbf{J}^\top \nabla_z \log \pi_\theta(o_0^{(S)}) \right\| > \frac{\hat{A}}{T_L} \rho_0^{(L)} \left\| \mathbf{J}^\top \nabla_z \log \pi_\theta(o_0^{(L)}) \right\| \end{aligned}$$

$\hat{A} > 0$ cancels out without changing the inequality's direction. Using the previous results, it deduces

$$\frac{\rho_0^{(S)}}{T_S} \left\| \mathbf{J}^\top (\mathbf{e}_{k_S} - \boldsymbol{\pi}_\theta) \right\| > \frac{\rho_0^{(L)}}{T_L} \left\| \mathbf{J}^\top (\mathbf{e}_{k_L} - \boldsymbol{\pi}_\theta) \right\| \quad (13)$$

From the singular value bounds for \mathbf{J} , we have

$$\sigma_{\min}(\mathbf{J}) \|\mathbf{v}\| \leq \left\| \mathbf{J}^\top \mathbf{v} \right\| \leq \sigma_{\max}(\mathbf{J}) \|\mathbf{v}\|,$$

where

- $\sigma_{\min}(\mathbf{J})$ is the smallest singular value,
- $\sigma_{\max}(\mathbf{J})$ is the largest singular value,
- $\kappa(\mathbf{J}) = \frac{\sigma_{\max}(\mathbf{J})}{\sigma_{\min}(\mathbf{J})}$ is the condition number of \mathbf{J} .

Using these bounds, inequality (13) can be written as

$$\frac{\rho_0^{(S)}}{T_S} \|\mathbf{e}_{k_S} - \boldsymbol{\pi}_\theta\| > \frac{\rho_0^{(L)}}{T_L} \tilde{\kappa} \|\mathbf{e}_{k_L} - \boldsymbol{\pi}_\theta\|.$$

where $\tilde{\kappa} \in [\kappa(\mathbf{J})^{-1}, \kappa(\mathbf{J})]$ is a constant. Substituting $f(k) := \|\mathbf{e}_k - \boldsymbol{\pi}_\theta\|$ from the previous part yields the claimed inequality and completes the second part of the proof.

Sufficient condition:

$$\frac{\rho_0^{(S)}}{T_S} \sigma_{\min}(\mathbf{J}) \|\mathbf{e}_{k_S} - \boldsymbol{\pi}_\theta\| > \frac{\rho_0^{(L)}}{T_L} \sigma_{\max}(\mathbf{J}) \|\mathbf{e}_{k_L} - \boldsymbol{\pi}_\theta\|$$

or equivalently,

$$\frac{\rho_0^{(S)}}{T_S} \|\mathbf{e}_{k_S} - \boldsymbol{\pi}_\theta\| > \frac{\rho_0^{(L)}}{T_L} \kappa(\mathbf{J}) \|\mathbf{e}_{k_L} - \boldsymbol{\pi}_\theta\|.$$

Necessary condition:

$$\frac{\rho_0^{(S)}}{T_S} \sigma_{\max}(\mathbf{J}) \|\mathbf{e}_{k_S} - \boldsymbol{\pi}_\theta\| > \frac{\rho_0^{(L)}}{T_L} \sigma_{\min}(\mathbf{J}) \|\mathbf{e}_{k_L} - \boldsymbol{\pi}_\theta\|$$

or equivalently,

$$\frac{\rho_0^{(S)}}{T_S} \|\mathbf{e}_{k_S} - \boldsymbol{\pi}_\theta\| > \frac{\rho_0^{(L)}}{T_L} \kappa(\mathbf{J})^{-1} \|\mathbf{e}_{k_L} - \boldsymbol{\pi}_\theta\|.$$

Remark that:

1. The necessary condition is almost trivial, since $\kappa(\mathbf{J})^{-1}$ can be very small, helping (13) to easily hold.
2. The sufficient condition is too strong and may not be needed.
3. In practice, (13) can hold with $\tilde{\kappa}$ significantly smaller than $\kappa(\mathbf{J})$.

Effect of Temperature. If the logits are scaled by temperature $\tau > 0$ before softmax:

$$\pi_\theta(k) = \frac{e^{z_k/\tau}}{\sum_{j=1}^K e^{z_j/\tau}},$$

then the gradient becomes:

$$\nabla_z \log \pi_\theta(k) = \frac{1}{\tau} (\mathbf{e}_k - \boldsymbol{\pi}_\theta),$$

and the norm scales as $1/\tau$. However, the form of the inequality and comparisons remain valid modulo this shared scaling, which concludes the last part of the Theorem.

A.6 Experimental Setup

For the PPO experiments, we used the following reward scheme: +1 if the final answer was correct and enclosed in a box; -0.5 if the answer was boxed but incorrect; and -1 if no boxed answer was provided. During training, we set $\gamma = 1$ and $\lambda = 0.95$. For each input, the model generated 8 samples using a temperature of 0.6 and $\text{top}_p = 1$, with a maximum sequence length of 20,000 tokens. We used the Adam optimizer with a learning rate of 5×10^{-7} for the actor and 9×10^{-6} for the critic.

For GRPO experiments, we used a +1 reward for a correct and boxed final answer, and a 0 reward otherwise. During training, we set $\gamma = 1$. For each input, the model generated 8 samples using a temperature of 0.6 and $\text{top}_p = 1$, with a maximum sequence length of 24,576 tokens. We used the Adam optimizer with a learning rate of 1×10^{-6} for the actor.

A.7 Compute Resources

The experiments were conducted using H100 GPUs for compute. The training was done using 8 GPUs, with each GPU having 80 GB of memory, and sufficient storage to accommodate the dataset and model checkpoints. The second-stage post-training of R1 models required fewer than 60 training steps and took approximately 19 GPU hours for the 1.5B model and 41 GPU hours for the 7B model.

A.8 Stable Training of PPO with $\lambda < 1$

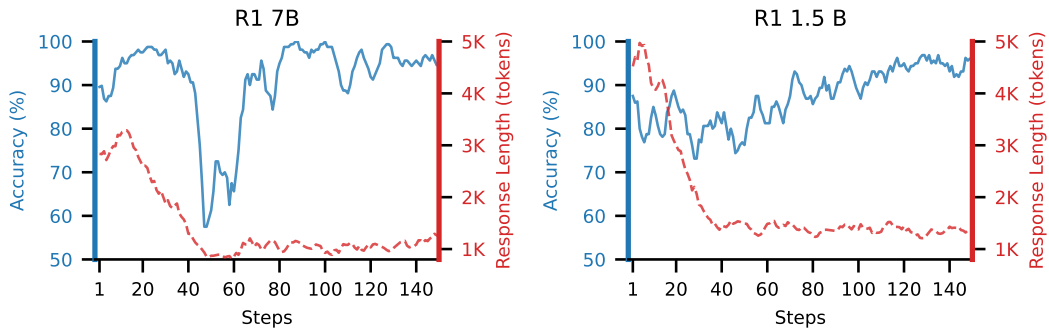


Figure 5: Reinforcement learning is performed using PPO algorithm with 8 example and $\gamma = 1$ on two base models: *DeepSeek-R1-Distill-Qwen-1.5B* (right) and *DeepSeek-R1-Distill-Qwen-7B* (left). The examples are randomly selected from level-5 questions of the MATH dataset. The plots illustrate average accuracy and length of generated responses during the PPO training.

A.9 Unstable Training of PPO with $\lambda = 1$

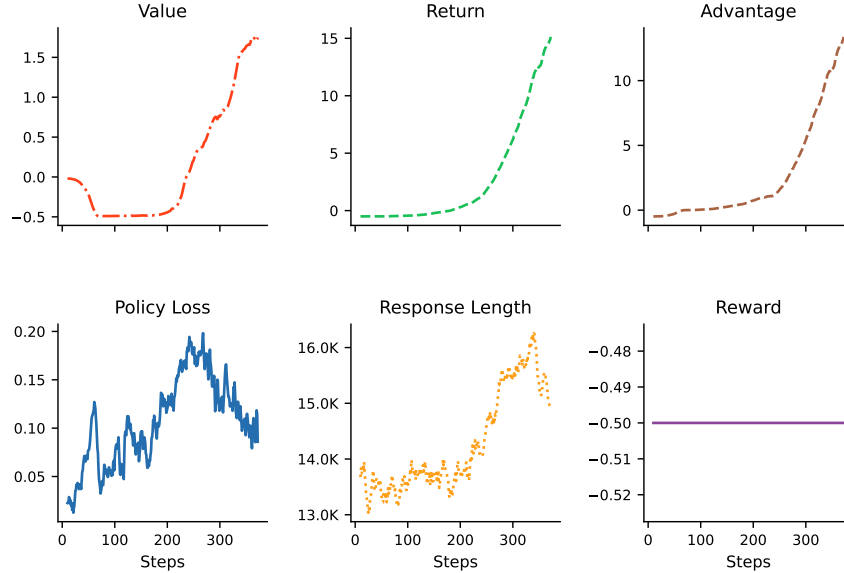


Figure 6: PPO training was conducted with $\lambda = 1$ on four problems selected from the OlympiadBench dataset. Notably, there is an exponential **return overflow** starting around step 100. Importantly, the reward consistently *remains at -0.5 over all the training steps*.

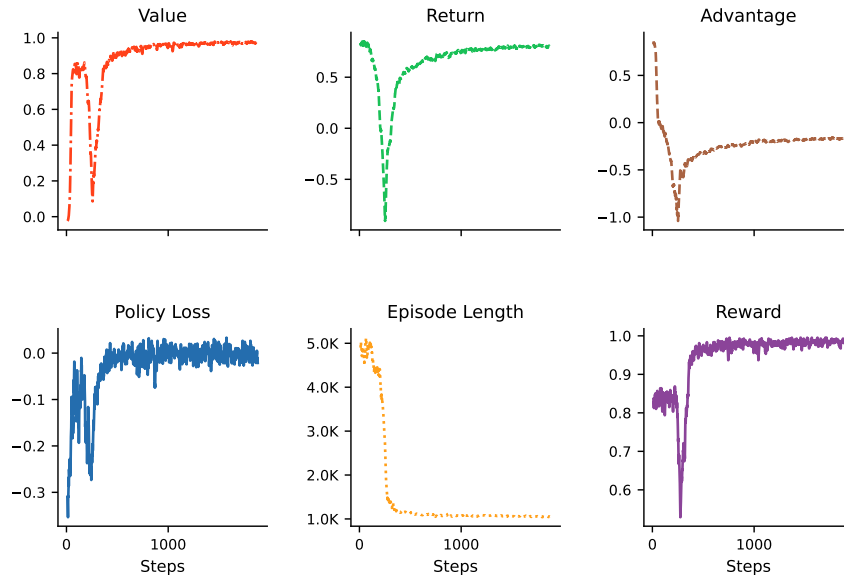


Figure 7: PPO training with $\lambda = 1$, conducted on four problems selected from the MATH dataset, which are somehow solvable. **Return underflow** starts early, but almost quickly stops. Nonetheless, while the response length decreases, it still requires **significantly more steps** to achieve this compared to similar training with $\lambda < 1$ (e.g., compare it to Figure 5 where in only ~ 40 steps, the model achieves similar length reduction).

A.10 GRPO training on MATH examples

Figure 8 illustrates the accuracy and response length of DeepSeek-R1-Distill-Qwen-1.5B over training steps trained with GRPO using eight training examples from the training subset of MATH dataset and, evaluated on different *test* datasets, AIME 2024, AMC 2023, and MATH-500. For evaluation, we generated four samples per query using a temperature of 0.6 and top-p of 0.95. In the first half of the steps, response length decreased while accuracy remained stable or improved across benchmarks. In the second half, both response length and accuracy showed fluctuations, indicating unstable performance.

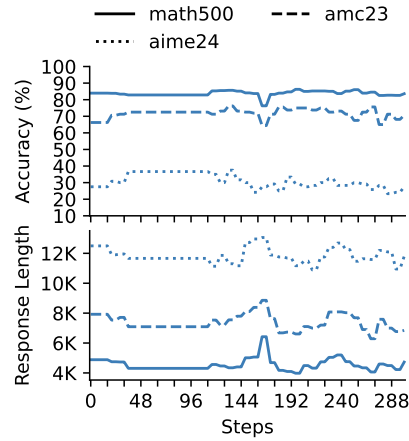


Figure 8: Response dynamics of *DeepSeek-R1-Distill-Qwen-1.5B* trained with GRPO using 8 problems from the level-5 subset of MATH dataset evaluated on three mathematics benchmarks (different line styles).